The Seasonal Cycle of Blocking and Associated Physical Mechanisms in the Australian Region and Relationship with Rainfall

M. J. POOK, J. S. RISBEY, AND P. C. MCINTOSH

CAWCR CSIRO Marine and Atmospheric Research, Hobart, Tasmania, and Climate Adaptation National Research Flagship, Clayton, Victoria, Australia

C. C. UMMENHOFER*

Climate Change Research Centre, University of New South Wales, Sydney, Australia

A. G. MARSHALL

CAWCR Bureau of Meteorology, Hobart, Tasmania, Australia

G. A. MEYERS

CSIRO Marine and Atmospheric Research, Hobart, Tasmania, Australia

(Manuscript received 24 January 2013, in final form 23 July 2013)

ABSTRACT

The seasonal cycle of blocking in the Australian region is shown to be associated with major seasonal temperature changes over continental Antarctica (approximately 15°–35°C) and Australia (about 8°–17°C) and with minor changes over the surrounding oceans (below 5°C). These changes are superimposed on a favorable background state for blocking in the region resulting from a conjunction of physical influences. These include the geographical configuration and topography of the Australian and Antarctic continents and the positive west to east gradient of sea surface temperature in the Indo-Australian sector of the Southern Ocean. Blocking is represented by a blocking index (BI) developed by the Australian Bureau of Meteorology. The BI has a marked seasonal cycle that reflects seasonal changes in the strength of the westerly winds in the midtroposphere at selected latitudes. Significant correlations between the BI at Australian longitudes and rainfall have been demonstrated in southern and central Australia for the austral autumn, winter, and spring. Patchy positive correlations are evident in the south during summer but significant negative correlations are apparent in the central tropical north. By decomposing the rainfall into its contributions from identifiable synoptic types during the April–October growing season, it is shown that the high correlation between blocking and rainfall in southern Australia is explained by the component of rainfall associated with cutoff lows. These systems form the cyclonic components of blocking dipoles. In contrast, there is no significant correlation between the BI and rainfall from Southern Ocean fronts.

1. Introduction

Atmospheric blocking is broadly recognized by synopticians as a situation where a synoptic-scale anticyclone becomes quasi stationary well poleward of the mean subtropical ridge position for the particular time of year. More specifically in the Australian region, it presents as a strongly involuted tropospheric flow pattern with a clearly defined split-jet structure. Blocking is one of the most significant phenomena encountered in the day to day weather cycle yet the prediction of its onset, duration, and dissipation in numerical weather prediction (NWP) remains problematic at the medium-range time scale (Watson and Colucci 2002; Renwick 2005). Furthermore, the problem of prediction becomes more challenging in coupled general circulation models (GCMs)

* Current affiliation: Department of Physical Oceanography, Woods Hole Oceanographic Institution, Woods Hole, Massachusetts.

Corresponding author address: Dr. Michael Pook, CSIRO Marine and Atmospheric Research, GPO Box 1538, Hobart, TAS 7001 Australia.
E-mail: mike.pook@csiro.au

DOI: 10.1175/MWR-D-13-00040.1

run on the seasonal and longer time scales. Palmer et al. (2008) have demonstrated that the frequency of winter blocking is systematically underestimated in the Northern Hemisphere (NH) by a selection of these climate models. Similar detailed studies of the behavior of climate models in relation to blocking in the Southern Hemisphere (SH) have been undertaken recently (e.g., Ummenhofer et al. 2013; Marshall et al. 2013).

The main characteristics of atmospheric blocking in the SH have been examined in a range of studies (e.g., van Loon 1956; Coughlan 1983; Lejenäs 1984; Trenberth and Mo 1985; Sinclair 1996; Wiedenmann et al. 2002; Renwick 2005; O'Kane et al. 2013) while the associated winter split-jet pattern has been investigated by Bals-Elsholz et al. (2001). Studies with a specific concentration within the Pacific Ocean and the Australian and New Zealand region include those of Wright (1974), Hirst and Linacre (1981), Pook (1994), Renwick (1998), and Pook and Gibson (1999). Studies of the anticyclonic component of blocking patterns have tended to predominate even though Langford (1960) and Taljaard (1972) had included cutoff lows as part of the single phenomenon in their discussions of blocking. Wright (1974) contended that the cyclonic systems involved cannot be regarded as less important than the anticyclonic component.

The critical contribution to blocking onset and maintenance by topographical features was established by Charney and DeVore (1979) and expanded on by Gill (1982). He summarized results of several studies of the forcing of barotropic fluid flow that revealed the possibility of having two stable response patterns to the same forcing: one of strong zonal flow and a second involving subcritical flow that permits the formation and persistence of standing waves. More recently, Zidikheri et al. (2007) have examined blocking in terms of multiple equilibrium states of the midlatitude atmospheric circulation emphasizing the critical role of topography to blocking in the SH.

In the Australasian region, the fundamental questions concerning the initial development and subsequent persistence of blocking anticyclones have been posed by Baines (1983). He postulated that baroclinic instability represents the most likely mechanism for the initiation of blocking in the region while the maintenance of the blocked flow is best explained by a localized multiple equilibrium state associated with thermal forcing, probably by the sea surface temperature (SST) pattern. Frederiksen (1983) developed a three-dimensional instability theory that was able to capture the essential synoptic features of blocking in the Australian region when applied to the basic state of a SH wintertime synoptic flow field. He showed rigorously that baroclinic disturbances were associated with block initiation and decay and that barotropic disturbances were associated with maintaining the blocking structure. Majda et al. (2006) showed the critical role of higher-order turbulent processes in block initiation.

Blocking serves as an important ''driver'' of Australian weather and climate by influencing the suppression of rainfall in the regions dominated by the anticyclonic component while contributing to enhanced rainfall in the regions where the cyclonic components are located (Pook and Gibson 1999; Pook et al. 2006; Risbey et al. 2009b). An association of blocking with rainfall poses a paradox because periods of blocking often accompany extended dry spells in southern Australia, including Tasmania. By way of contrast, significant rainfall events are also known to occur over southern, eastern and inland Australia when high pressure systems dominate to the south or southeast of the continent (Foley 1956; Hill 1969; Mills and Wu 1995; Hopkins and Holland 1997; Griffiths et al. 1998; Qi et al. 1999; Pook et al. 2006). The explanation lies in the interactive relationship between the extensive high-latitude anticyclonic component of blocking on the one hand and the cutting off or isolation of a relatively small cyclonic component equatorward of the high. The resulting cutoff lows are known to be major contributors to rainfall events in the broad-acre agricultural areas of southern Australia and to runoff in Australia's major river catchments (Pook et al. 2006, 2009; Risbey et al. 2009a; Pook et al. 2010). In blocking episodes, the Southern Ocean cyclones on the poleward side of the highs tend to be steered to higher latitudes and in exceptional cases, have been observed to cross the circumpolar trough and produce precipitation over the high plateau of Antarctica (Pook and Cowled 1999; Massom et al. 2004). Figure 1 shows an example of a blocking anticyclone and associated cutoff low in the Australian region in April 2007. The near-vertical alignment of the main centers of mean sea level pressure (MSLP) and geopotential height at 500 hPa clearly demonstrates the equivalent barotropic nature of the structure.

It is well known that there tends to be a seasonal cycle of blocking with a preference in each hemisphere for higher frequencies of occurrence of blocking anticyclones within particular sectors (Hirst and Linacre 1981; Coughlan 1983; Lejenäs 1984; Trenberth and Mo 1985; Wiedenmann et al. 2002; O'Kane et al. 2013). This characteristic makes it desirable to examine the background physical conditions prevailing in a region and their variability in order to better understand the phenomenon. In this connection, the possible association of the frequency of atmospheric blocking with the marked west to east SST gradient over the Southern Ocean waters

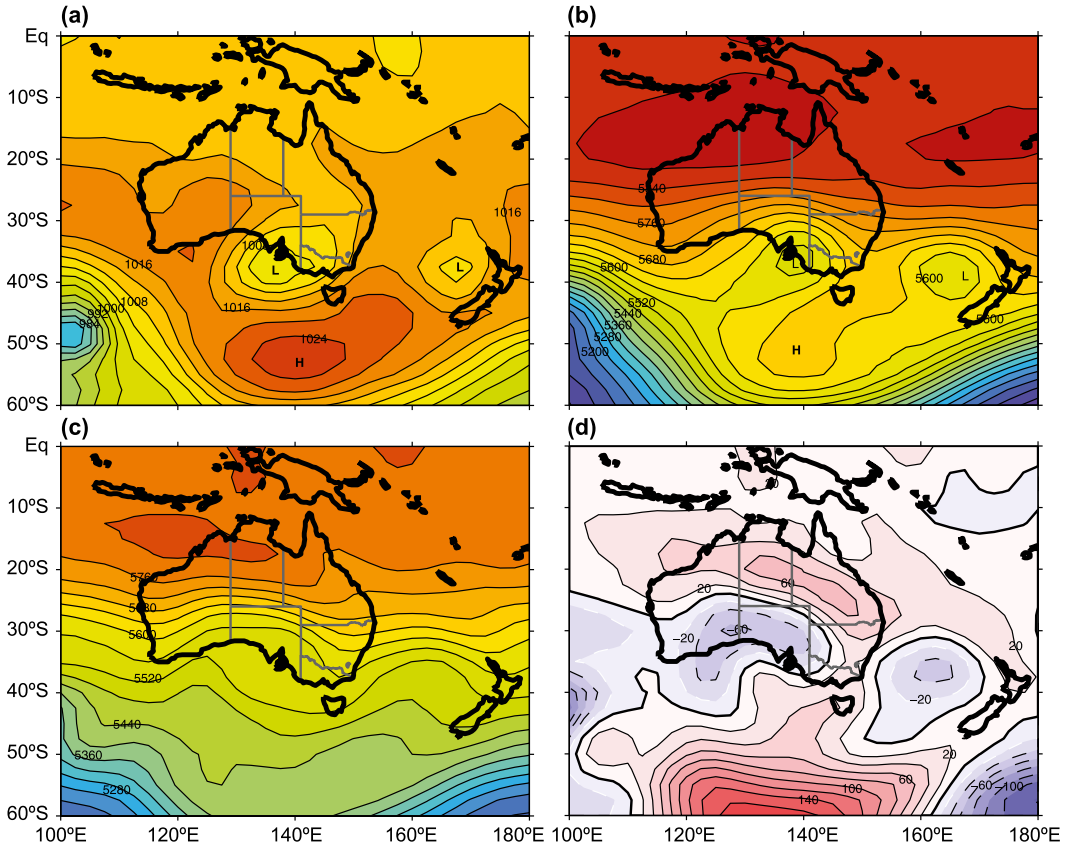

FIG. 1. A blocking pattern affecting southern Australia at 1200 UTC 27 Apr 2007 represented by fields of (a) MSLP, (b) 500-hPa geopotential, (c) 1000–500-hPa thickness, and (d) the 1000–500-hPa thickness anomaly. Red represents the highest values and blue represents the lowest values in each case. Dashed contours in (d) indicate negative values.

south of Australia between the cold Indian Ocean sector and the relatively warm Tasman Sea and southwest Pacific Ocean sector was first noted by Taljaard (1972). The concept was pursued by Wright (1974) in his detailed study of blocking frequency in the Australian region. Hirst and Linacre (1981) made reference to this possible association and also drew attention to an apparent semiannual cycle of blocking frequency in the Australian region, which was evident in the earlier data analysis of Wright (1974). Their tentative conclusions suggested that the west to east SST gradient along midlatitudes from the Indian Ocean to the Tasman Sea may be a factor in the high frequency of occurrence of blocking in the Tasman Sea–New Zealand region. Coughlan (1983) summarized this previous work and illustrated the magnitude of the SST gradient along 50°S in the Southern Ocean for the month of October in his Fig. 13. These authors did not explicitly propose a mechanism for the possible link with blocking nor did they relate the pronounced seasonal cycle of blocking activity to any seasonal cycle of SST or SST gradient. However, Pook (1994) showed the significant correlation between 1000–500-hPa thickness and SST along selected latitudes in the Indo-Australian sector of the Southern Ocean. This close relationship provides an explanation for the background atmospheric state of a dominant upper air trough over the cold waters to the southwest of Australia and a persistent meridional ridge over the warmer waters to the southeast of the continent, where the highest frequency of blocking in the region is observed.

In this paper, we examine the seasonal cycle of blocking in the Australian region within the context of the seasonal variability of the background temperature gradients over the Australian continent, the surrounding oceans, and Antarctica. In particular, the seasonality of the zonal and meridional SST gradients in the Indian Ocean and Australian region are identified. The observed temperature anomalies in the atmosphere are treated as the broad response to the atmosphere–surface interactions.

The paper is structured in the following manner. After a discussion of the phenomenon of blocking in section 1,

the data sources and methods used in our analysis are presented in section 2 and the measures used to identify blocking are compared in section 3. The general results of the analysis are in section 4 with an exploration of the relationships between blocking and rainfall in section 5. The conclusions are presented in section 6.

2. Data and methods

The atmospheric data used in the calculation of the various indices presented in this paper [including the Australian Bureau of Meteorology (BoM) blocking index (BI), Tibaldi–Molteni blocking index (TMBI), the zonal index (ZI), and 1000–500-hPa thickness] have been obtained from the National Centers for Environmental Prediction–National Center for Atmospheric Research (NCEP–NCAR) climate reanalysis (Reanalysis 1) dataset (Kalnay et al. 1996; Kistler et al. 2001). The NCEP–NCAR dataset consists of 4 analyses per day (at 6-hourly intervals from 0000 UTC) at a resolution of 2.5° latitude by 2.5° longitude for the standard atmospheric levels from the surface to the lower stratosphere. Monthly means of air temperature and geopotential have also been extracted from Reanalysis 1. Because of the well-known problems with data quality in the SH in the first decade of the NCEP–NCAR dataset (Kistler et al. 2001) this analysis has been confined to the period from 1958 to 2009. As discussed in Pook et al. (2012), upper air data had become widely available in the Australian region around the time of the International Geophysical Year (IGY; 1957–58) with approximately 30 radiosonde stations in operation (Bradshaw 1997). However, it should be noted that the ingestion of satellite soundings was not introduced until 1979 and there is some evidence that reanalysis quality in the SH may have been reduced in the first two decades of this analysis, particularly south of 50°S (Kistler et al. 2001). Monthly mean SST data for the SH were extracted from the Hadley Centre Sea Ice and Sea Surface Temperature dataset (HadISST; Rayner et al. 2003).

Rainfall data for individual stations have been obtained from the Patched Point Dataset supplied by the Queensland Department of Science, Information Technology, Innovation and the Arts (Jeffrey et al. 2001) to provide a consistent technique to insert estimates of missing data. The Patched Point Dataset uses original BoM measurements for a particular meteorological station but interpolated data are inserted to fill any gaps in the observation record. The gridded rainfall and surface temperature data have been derived from the 0.05° × 0.05° Australian Water Availability Project (AWAP) monthly dataset (version 3) for the period 1900–2009 (Jones et al. 2009).

Indices of blocking activity were designed in the first instance to detect, quantify, and separate individual episodes of blocking. Blocking episodes or events typically persist for periods of several days out to a week or so in the SH (Wright 1974; Coughlan 1983; Trenberth and Mo 1985; Pook and Gibson 1999; Wiedenmann et al. 2002). However, the use of indices has also been extended to assume a role in identifying anomalies of blocking in a given region over monthly and seasonal time scales (see e.g., Ohis 1980; Tobin and Skinner 2012).

After comparing the effectiveness of a selection of daily indices, we investigate the monthly cycle of blocking by employing mean blocking indices for each month on the assumption that the monthly means reflect the underlying predisposition to blocking in a particular month. It is possible to conceive of situations in which high and low blocking tendencies at different periods cancel out on the monthly time scale. However, over the averaging period of the five decades employed here for the monthly data it is argued that the seasonal cycle is accurately reflected. We test this assertion by correlating the monthly mean of the BI at 140°E with the number of days in the month when the BI on one or more synoptic hours was a minimum of one standard deviation above the long-term mean for that month. Figure 2 shows that there is a close relationship between the number of days where flow is blocked according to this threshold and the individual monthly mean of the BI in each of the months chosen to represent the seasons.

The seasonal cycles of SST, continental surface air temperature, and atmospheric 1000–500-hPa thickness were computed and compared with the cycle of blocking. Finally, composites of background SST, air temperature, rainfall, and atmospheric thickness were constructed in years of high (low) blocking where the average normalized BI anomaly was at least + (−) one standard deviation. The main period of interest for rainfall in this study is the standard growing season for winter crops in southern Australia, which extends from April to October (Pook et al. 2006, 2009, 2012).

3. Measures of blocking activity in the Australian region

a. Blocking definitions

Although several differences have been identified between the characteristics of blocking in the NH and the SH (Coughlan 1983), it was inevitable that early studies of blocking in the SH would follow the approaches adopted in the north. In the NH, Rex (1950) was able to take advantage of the upper air network, which had been established by the middle of the twentieth century

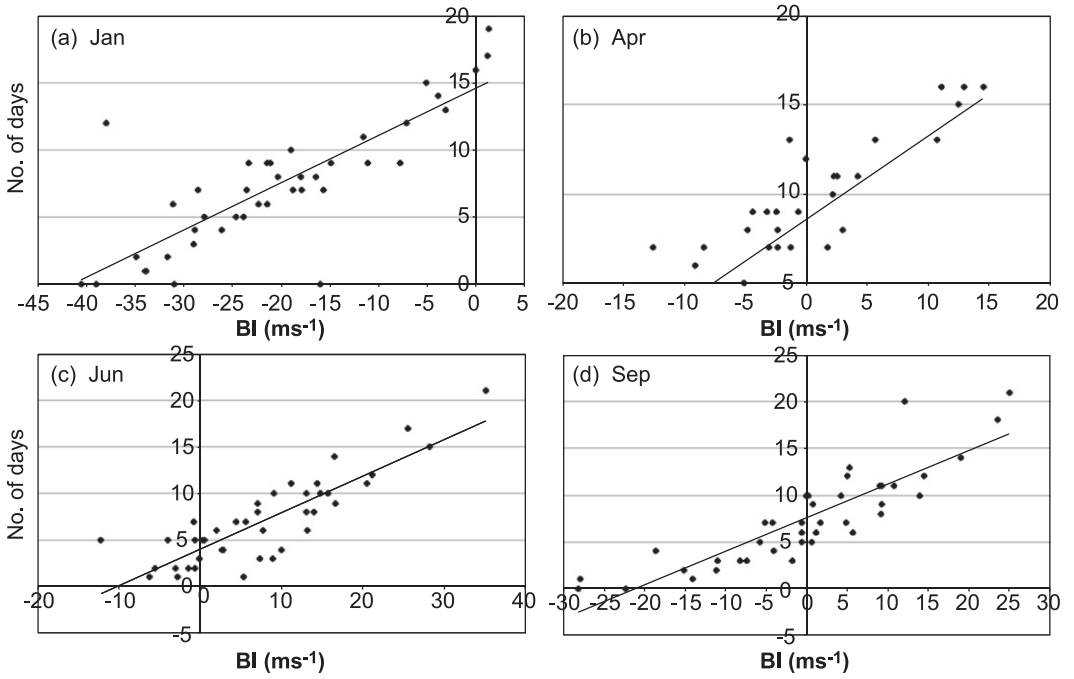

FIG. 2. Scatterplots showing the monthly means of the Australian Bureau of Meteorology BI at 140°E (*x* axis) vs the number of days in the month when the BI is ≥1 standard deviation above the long-term mean (*y* axis) with estimated lines of best fit for (a) January, (b) April, (c) June, and (d) September. The BI is defined in Eq. (1).

in order to define five necessary concurrent conditions for an atmospheric block to occur. However, owing to the unavailability of comprehensive upper air data for the SH, van Loon (1956) developed a set of three basic requirements for satisfactorily defining a blocking situation from MSLP data only. Subsequently, Wright (1974) had access to the upper air data, which Bradshaw (1997) reports had been established in the Australian region by the time of the IGY.

Wright (1974) developed an alternative definition of blocking to that of van Loon (1956) in order to take account of the occurrence of a "process which may be called one of displacement and replacement" (Wright 1974, p. 3). In this expression of blocking action an individual MSLP high pressure center was free to weaken and move northeastward only to be replaced from the west by another anticyclone of similar strength. Meanwhile, the upper air ridge remained clearly identifiable and confined to a narrow range of longitudes during the entire blocking episode which was required to last for at least six days. Alternative techniques for the identification of blocking have largely been based on calculation of anomalies in the geopotential height fields. Examples of this approach include Charney et al. (1981) in the NH and Trenberth and Mo (1985) for the SH.

In a novel approach, O'Kane et al. (2013) compared nonstationary cluster analysis techniques to blocking indices in order to identify separate metastable regimes in the SH atmospheric circulation. Their analysis reveals positive and negative phases of a hemispheric midlatitude blocking state prior to 1978 and a transition state identified with the southern annular mode (SAM). In recent decades the SAM has replaced the negative phase of blocking as a metastable state in its own right and the dominance of the positive blocking pattern has gradually decreased.

b. Blocking indices

To provide an objective identification of blocking events in the Australian region Wright (1974) advocated the application of a flow-based BI, which was developed by the Extended Forecast Section of the Australian BoM. The original form of the BI estimated the difference at 500 hPa between the sum of the geostrophic westerly wind components (U components) at a relatively low latitude (27.5°S) and a high latitude (57.5°S) and the sum of the U components at 42.5° and 47.5°S. The U components were calculated from the 5-day mean fields of geopotential height (Wright 1974). In the early 1990s, the index was modified in an apparently undocumented internal change to arrive at its current form (Pook and Gibson 1999) of

$$\mathrm{BI} = 0.5(U_{25} + U_{30} + U_{55} + U_{60} - U_{40} - U_{50} - 2U_{45}), \quad (1)$$

where at a given meridian U_x represents the zonal component (U component) of the mean 500-hPa geostrophic wind at latitude x (°S). Hence, the index measures the relative influences of the U components of the geostrophic wind at mid-, high, and low latitudes. High values of BI indicate situations in which the high- and low-latitude westerly winds are strong or the midlatitude westerly flow is weak, or a combination of both. Split-flow configurations of this type correspond to blocking activity but the index is unable to convey information on the degree of meridionality of the flow or the latitudinal separation of the zonal wind maxima.

Lejenäs (1984) employed a ZI defined in terms of the geopotential height difference at the 500-hPa level between 35° and 50°S to measure the incidence of blocking in the SH. Negative values of the index for a specific meridian together with negative mean values of the index over the 30° of longitude centered on that meridian are taken as specifying blocking on a given day. Lejenäs (1984) concluded from his analysis that blocking does not occur as frequently in the SH as in the NH and that there is one preferred region for blocking in this hemisphere; the Pacific sector east of Australia.

Tibaldi et al. (1994) adapted and modified a blocking index that had been developed for the NH (see Tibaldi and Molteni 1990) in order to identify blocking in the SH. Based on a dataset of seven years of European Centre for Medium-Range Weather Forecasts (ECMWF) data from December 1980 to November 1987, Tibaldi et al. (1994) prescribed two conditions that had to be met in order for ''blocked flow'' to be diagnosed at a meridian. A low-latitude geopotential difference at 500 hPa (designated GHGN) was calculated between primary latitudes of 35° and 50°S as in Lejenäs (1984) and a high latitude geopotential difference (GHS) was calculated between 50°S and a southern latitude of 65°S. However, Tibaldi et al. (1994) allowed for slight variations in the primary latitudes in order to obtain maxima in values of the index. The index can be summarized in the following manner:

$$\mathrm{GHS} = \frac{z(\phi_S) - z(\phi_0)}{\phi_S - \phi_0}; \quad \mathrm{GHGN} = \frac{z(\phi_0) - z(\phi_N)}{\phi_0 - \phi_N}, \qquad (2)$$

where $\phi_N = 35°\mathrm{S} + \Delta$, $\phi_0 = 50°\mathrm{S} + \Delta$, $\phi_S = 65°\mathrm{S} + \Delta$, and $\Delta = (-3.75°, 0°, +3.75°)$.

There are two conditions that have to be met for at least one value of Δ in order to define blocking at a particular meridian. These are: GHGN > 0 and GHGS < -10 m per degree of latitude. In this study we have used $\Delta = (-2.5°, 0°, +2.5°)$, which is the NCEP–NCAR Reanalysis 1 gridpoint interval. This index has been identified as TMBI.

4. Results

a. Comparison of blocking indices

A comparison of the BI and TMBI indices for an extended period of significant blocking identified in 1989 by Pook (1994) is shown in Fig. 3. Additionally, the 5-day mean geopotential height at 45°S is included in the comparison as this is the second criterion of the definition of blocking proposed by Wright (1974). Figure 3 indicates that the 5-day mean of the BI and the daily mean of the TMBI identify similar periods of blocking for the most part but the TMBI has more stringent requirements and hence does not register the event confined between 120° and 140°E in mid-June (Fig. 3b) and the more significant event centered in the second half of August (dashed arrow) as blocking situations. On the other hand, the 500-hPa mean geopotential at 45°S does not capture some of the major events identified by TMBI and BI, at all. This is especially apparent for the event in mid-July 1989, which is marked by the full arrow in Fig. 3.

Figure 4 reveals that the conditions required to be met by the TMBI in order to specify blocked flow at a meridian (here 140°E) at a given synoptic time are relatively rarely met during the June–November period. According to the TMBI, blocked flow is achieved at 140°E on 7.4% of synoptic analyses in June (the maximum month for blocking), 6% in July, and 5% in May but 3% or less in every other month. By way of contrast a value of the BI of at least 40 m s^{-1} occurs on 10% of occasions in June and 9% in July and has a higher frequency of occurrence than the TMBI for all months except January, February, March, and December. Furthermore, a restriction in the use of the TMBI is the requirement that the stringent qualifying conditions need to be maintained for at least 5 days. Application of this time condition further significantly reduces the occurrence of blocking events according to this measure. By way of comparison, the cluster analysis of O'Kane et al. (2013) found that the characteristic blocking persistence is 3–4 days in the SH. The second restriction applying to the TMBI is that it takes no account of the cyclonic portion of the block unlike the BI, which measures the comparative strength of the subtropical and polar wind maxima. Significantly, Watson and Colucci (2002) found it necessary to modify the original TMBI in order to specify a midlatitude component in their NH study. Barriopedro et al. (2006) have made further modifications to the TMBI in order to develop an automated blocking detection technique from which a 55-yr blocking climatology has been derived for the NH. Schalge et al. (2011) have applied filters of intensity, zonal extent, and persistence to analyses using the TMBI in order to exclude cutoff lows and subsynoptic-scale

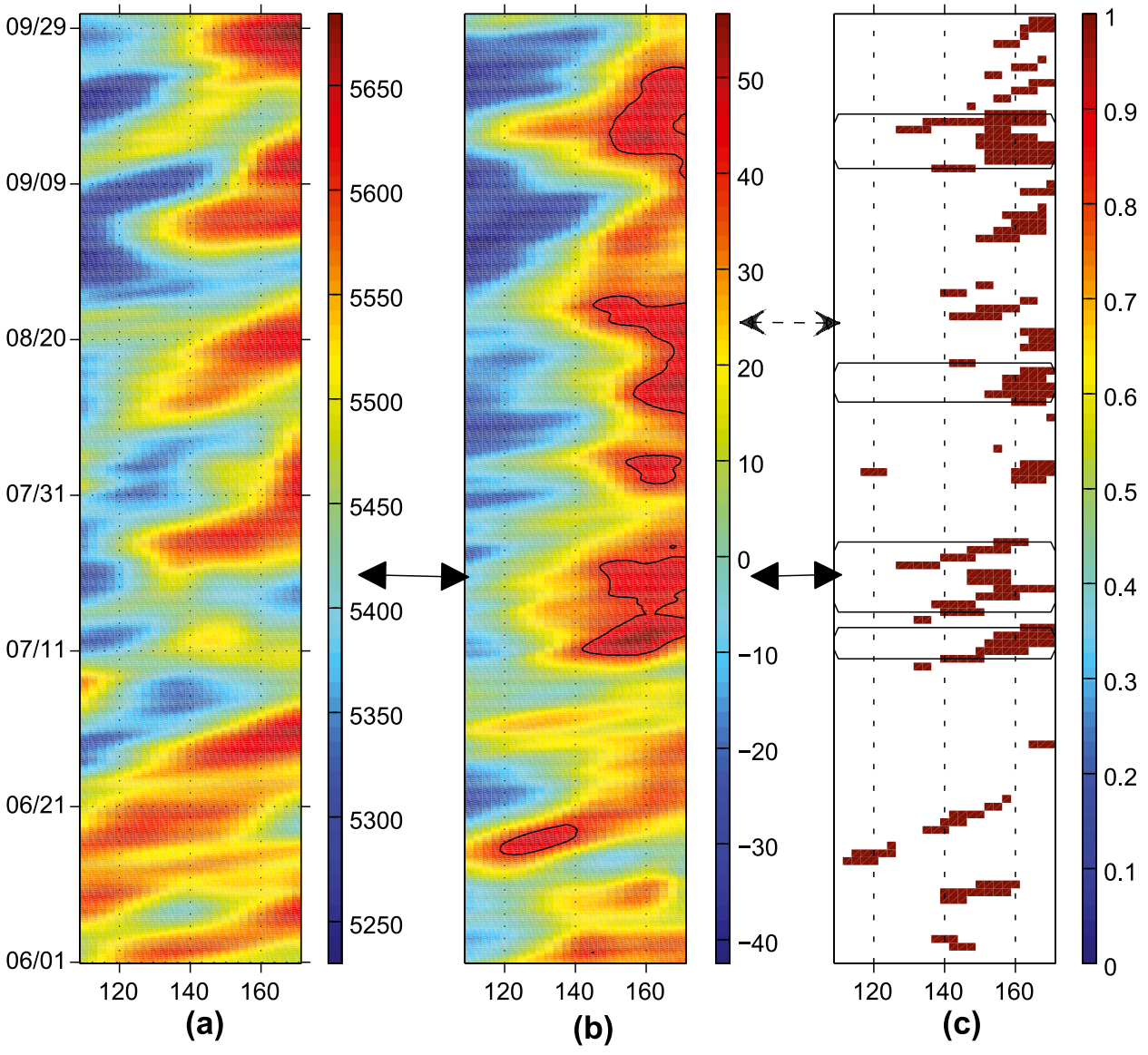

FIG. 3. Comparison of three measures of blocking activity in the Australian region over the period from 1 Jun to 30 Sep 1989: (a) the 5-day running mean of the 500-hPa geopotential height at 45°S, (b) the 5-day running mean of the Australian Bureau of Meteorology BI with the black contour marking the 40 m s^{-1} isopleth, and (c) the daily measure of the Tibaldi–Molteni index of blocked flow. The brackets in (c) mark periods when the 5-day condition for a block was met. The closed and open arrows refer to separate periods discussed in the text.

features that resemble blocking. In the SH component of their study, Schalge et al. (2011) report that a period of 3 days represents a sufficient minimum for the persistence filter.

In arguing the relative strengths of the blocking indices, it should be noted that the TMBI identifies a higher frequency of blocking in the austral summer at 140°E than the BI suggests (Fig. 4). This may be partly explained by the fact that Tibaldi et al. (1994) reported that the TMBI showed only a weak seasonal cycle for what the authors described as the ''Australian sector'' (between 150°E and 150°W). However, this sector is located to the east of the Australian continent and would more accurately be described as the New Zealand sector. It is eastward of the focus of this paper. Additionally, the extent of this sector (60° of longitude) is so great that it masks the identifiable seasonal changes in blocking frequency that have been detected to propagate eastward within it (Hirst and Linacre 1981). Nevertheless, because of the very large changes in the mean BI brought about by the seasonal changes in the background circulation (see section 4b), it is possible that the

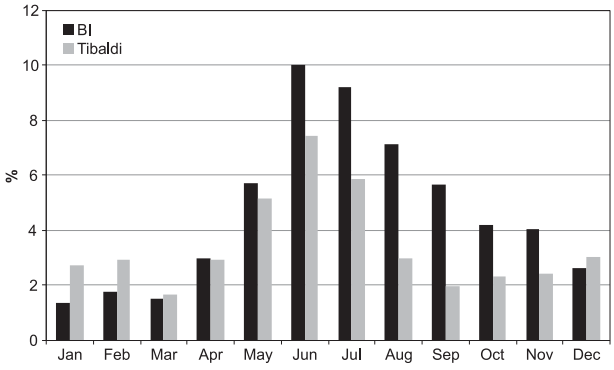

FIG. 4. The percentage frequency of the BI at 140°E reaching at least 40 m s^{-1} (black) and the percentage frequency of the Tibaldi–Molteni blocked flow condition being met at 140°E (gray) from NCEP–NCAR Reanalysis 1 6-hourly data. The period of analysis extends from January 1970 to December 2009.

TMBI gives a better measure of Australian blocking frequency in the summer months. Despite this exception, the ease of calculation of the BI and the history of its application in the region justify its use as the basic index for measurement of blocking in the remainder of this paper.

b. *The seasonal cycle of the BI*

Although the BI adequately measures individual blocking events throughout the march of the seasons, the monthly mean BI exhibits a marked seasonal cycle as the strength and location of the major midtropospheric wind maxima vary from summer to winter. The annual cycle of the BI at selected meridians from 120°E to the date line is indicated in Fig. 5a. There is a clear maximum at all meridians in winter, reflecting the well-known split in the upper-tropospheric westerly winds at that time of year (Trenberth and Mo 1985; Bals-Elsholz et al. 2001). The maximum value of the index occurs in June at 120°E, in July from 140° to 160°E, and in August at 180°. The eastward progression of the BI peak across Australia coincides with the continental surface cooling and decreasing atmospheric thickness discussed in the following section. A secondary maximum is identifiable in November at 120°E but there is no evidence in our analysis of this double maximum at the other meridians. This result contrasts with the findings of Hirst and Linacre (1981). However, their conclusion was based on frequency of occurrence of blocking events from the limited dataset of Wright (1974). By way of comparison, a measure of the geopotential gradient between 35° and 55°S, exhibits a seasonal cycle that is comparable with the BI results in Fig. 5a. Lejenäs (1984) and Tibaldi et al. (1994) measured the relative geopotential height difference between 35° and 50°S. In Fig. 5b, the difference in geopotential (delta *Z*) at 140°E between 35° and 55°S, the latitudes adopted in Pook (1992), provides an adequate representation of the seasonal cycle of the meridional gradient for the purposes of comparison with the BI. Figure 5b shows that the maximum in BI at 140°E corresponds to the minimum in delta *Z*. However, in summer, the minimum value of BI occurs in January while delta *Z* peaks in February.

Figure 5b has similar features to that shown by Pook (1992) in his Fig. 2, based on monthly means of a local zonal index at 500 hPa for a broad Australian sector extending from 75°E to 175°W. A simple hemispheric index of a similar form was developed by Gong and Wang (1999) based on the difference between normalized zonal means of MSLP at 40° and 65°S in order to obtain a measure of the large-scale shifts in mass between the mid- and high latitudes that occur in association with the SAM. Meneghini et al. (2007) produced an Australian regional index of the SAM that they found was more closely associated with the regional circulation and rainfall variability in parts of southern Australia than the hemispheric index.

The large seasonal cycles in BI and delta *Z* suggest that significant changes in atmospheric characteristics occur throughout the year and it is instructive to investigate the corresponding changes in continental and oceanic characteristics.

c. *The continental temperature cycle*

Figure 6 shows that the large Australian continent is positioned in the eastern region of the SH with the vast, elevated, and pole-centered continent of Antarctica to its south. East Antarctica extends farther north than any other portion of Antarctica except for the isolated, narrow extension of the Antarctic Peninsula near South America (not shown). The northernmost extent of the coastline in the Australian sector of East Antarctica is about 66°S and the average elevation inland of the coastal zone is over 2 km with highest elevations near 80°S, resulting in an asymmetric influence on the atmospheric flow in the SH (King and Turner 1997). Walsh et al. (2000) found in their modeling study that the topography of Antarctica has a major influence on baroclinicity over the ocean surrounding Antarctica and removal of the topography in their simulations greatly affected the mean flow.

The surface temperature change from summer to winter over the high plateau of continental Antarctica is of the order of 30°–35°C and the so-called coreless winter then persists from about April to September (King and Turner 1997; Bromwich and Parish 1998). Near the coast, the summer to winter temperature change is typically half that encountered on the plateau (King

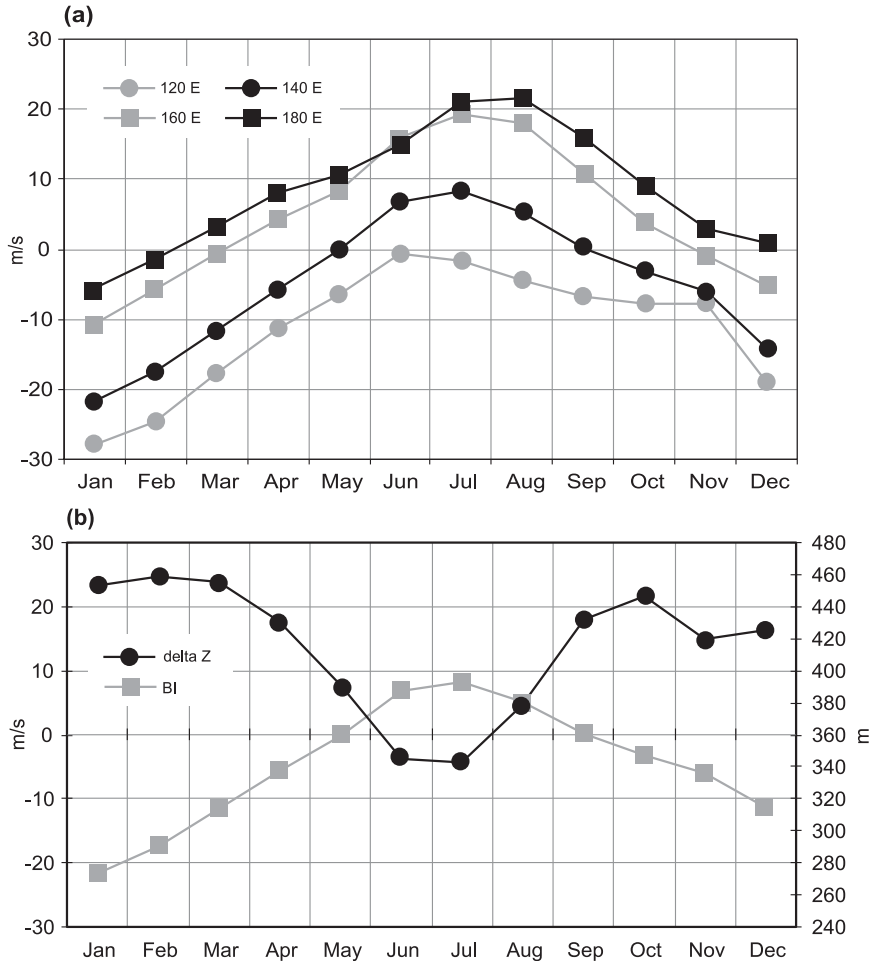

FIG. 5. (a) The seasonal cycle of the BI at selected meridians in the Australian region, and (b) the seasonal cycle of the BI at 140°E compared to the seasonal cycle of the difference in geopotential height (delta Z) between the mean geopotential heights at 35° and 55°S. The period is during 1958–2010.

and Turner 1997). Interestingly, mean temperature changes of a similar order to Antarctic coastal regions are also experienced over the central and southern parts of continental Australia (Gentilli 1971). Figure 7 shows the change in mean surface air temperature over Australia from summer [December–February (DJF)] to winter [June–August (JJA)]. The mean temperature is defined as one-half of the sum of the maximum (Tmax) and minimum (Tmin) temperatures and has been obtained from the dataset of Jones et al. (2009). The response in the atmospheric column to these surface temperature changes is reflected in large decreases in the 1000–500-hPa thickness over southern Australia and near the Antarctic coast with a corresponding change in the U component of the thermal wind from summer to winter. Figure 8 traces the seasonal changes in 1000–500-hPa thickness. Outside Antarctica, the steady contraction of the atmospheric column continues from autumn to winter (Fig. 8c) throughout the SH but is most obvious over the southern regions of the major continents. The cooling signal has its greatest geographical extent over the Australian region and results via thermal wind changes in a major reorganization of the jet streams from summer to winter. Figure 9 reveals the consequent changes in the U component of the 500-hPa wind over eastern Australia (140°E) from summer to winter at the latitudes used in the calculation of the BI. Each of the changes shown in Fig. 9 except for the negligible decrease in the U_{55} term, acts to increase the magnitude of the BI in winter.

Overall, the major changes in the land–sea temperature contrast between southern Australia and the surrounding oceans from summer to winter originally identified by Taljaard (1972) lead to changes in circulation

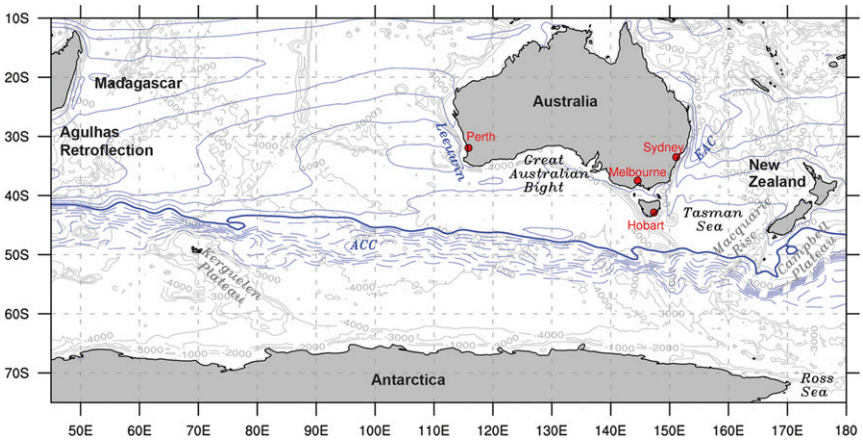

FIG. 6. Map of the study region, with key oceanographic/geographic features indicated. The gray bathymetry is based on the General Bathymetric Chart of the Oceans (GEBCO) and the blue contours on the Simple Ocean Data Assimilation (SODA) (Carton and Giese 2008) sea surface height, averaged for the period January 1958–December 2008, with a thick zero contour and contour intervals of 0.125 m.

in the upper air most clearly characterized by the enhancement of a ''split'' in the westerly flow over the Tasman Sea and New Zealand region. The split in the westerlies forms in response to this marked cooling of the atmospheric column over the Australian continent and the intensification of the meridional ridge (poleward of 40°S) at approximately 165°E. This ridge forms part of the dominant long wave in the westerlies over the Australian sector with the northeastward tilting trough anchored near 105°E at 40°S. Coughlan (1983) has identified the eastward tilt of the trough with decreasing latitude as favorable for transferring momentum into the subtropical jet.

The continental cooling in winter is accompanied by the intensification and equatorward movement of the subtropical jet stream to about 30°S, while the subtropical ridge in the lower atmosphere moves to its northernmost position (Radok 1971; Sturman and Tapper 1996; Hurrell et al. 1998), and a general weakening of the midtropospheric westerlies occurs in the midlatitudes. The persistence of the meridional ridge to the southeast of Australia corresponds with a maximum frequency of occurrence of atmospheric blocking in the region (Trenberth and Mo 1985; Pook 1994; Bals-Elsholz et al. 2001), which is reflected in the increase in the mean value of the BI in winter. According to Coughlan (1983), the Australasian region is unique in the SH as enhanced zonal wavenumbers from 1 to 4 are each characterized by midlatitude ridges south of 40°S at these longitudes in all seasons while tilted troughs occur at low latitudes in the same band. This configuration is particularly favorable for blocking action there. Wavenumber 3 dominates in the other preferred blocking regions of the hemisphere (Coughlan 1983).

A rapid reversal to warming and increasing atmospheric thickness occurs from winter to spring (Fig. 8d) and from spring to summer (Fig. 8a). The resulting changes in thermal wind in the Australian region give rise to a decline in the mean strength of the subtropical jet stream and increases in the zonal westerly wind in the midlatitudes. Figure 10 contrasts the mean westerly wind components at 140°E at the latitudes determining the BI in July and October. The changes from July to October act to decrease the contributions to the BI at low and midlatitudes but there are slight increases in the westerly wind components at the two high latitudes (55° and

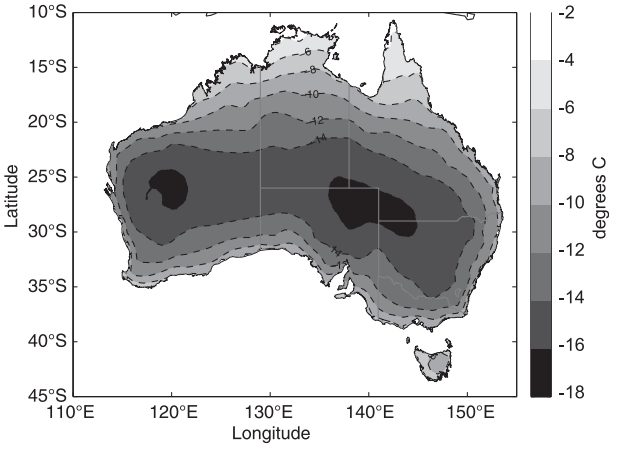

FIG. 7. The change in mean surface air temperature [(Tmax + Tmin)/2] across Australia from summer (DJF) to winter (JJA). The data period is from 1958 to 2009 from AWAP (Jones et al. 2009). Dashed lines indicate negative values.

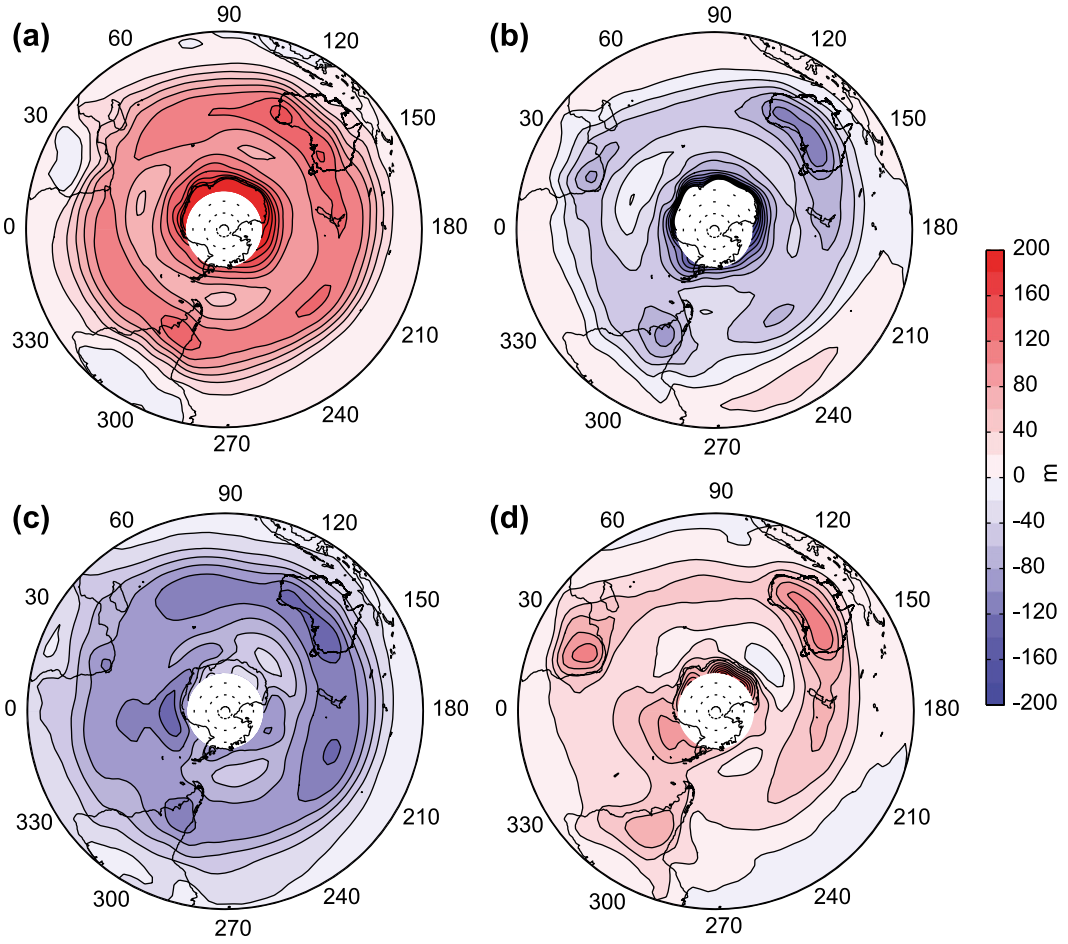

FIG. 8. The change in 1000–500-hPa thickness (m) from (a) October (spring) to January (summer), (b) January to April, (c) April to July, and (d) July to October over the Southern Hemisphere. Red shading represents positive changes and blue shading represents negative changes. The white area centered on the South Pole marks the high plateau of Antarctica where the elevation generally exceeds 2000 m. (NCEP–NCAR Reanalysis 1 data are for the period during 1958–2009.)

60°S) in the index. This behavior is explained by the fact that the sea ice around Antarctica is at its maximum extent in September and only begins its seasonal contraction in October (King and Turner 1997). Thus, there is little change in temperature in this region between winter and spring.

d. The oceanic temperature cycle

Although the largest seasonal changes in surface temperature are associated with the continents, the land areas occupy only a small proportion of the SH, particularly in the midlatitudes. Hence, seasonal changes in atmospheric temperature are largely related to seasonal changes in SST. Isotherms of mean SST in the SH are shown for each of the seasons in Fig. 11. Significant features of the SST structure in all seasons include the poleward extensions of warmer waters in the East Australia Current (EAC) and the Agulhas Current on the African east coast. The atypical poleward extension of warmer water off the west Australian coast (eastern boundary of the Indian Ocean) in Figs. 11a–c is evidence of the effect of the Leeuwin Current (see Fig. 6). In all seasons, the maximum meridional gradients of SST appear in the western Indian Ocean sector where the retroflection of the Agulhas Current interacts with the component of the Antarctic Circumpolar Current (ACC) confined to the equatorward side of the Kerguelen Plateau (e.g., Nowlin and Klinck 1986). South of about 45°S, SST are lower in the Indian Ocean sector than in the southwestern Pacific at similar latitudes resulting in the marked west to east SST gradient over the waters south of Australia previously discussed in section 1.

However, Pook (1994) was able to show that this west to east gradient of SST displays a seasonal cycle with the

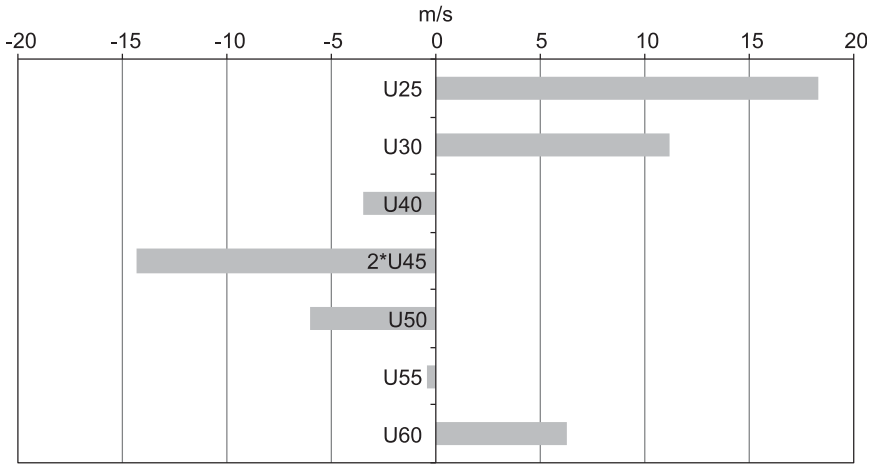

FIG. 9. The change in the mean U component of the 500-hPa wind ($m\,s^{-1}$) from January (summer) to July (winter) on the 140°E meridian at the latitudes employed in the calculation of the BI. Note that the value at 45°S has been doubled in order to match the term in the BI formula [see Eq. (1)]. (NCEP–NCAR Reanalysis 1 data are for the period during 1958–2009.)

maximum gradient occurring in the Australian sector in October. Figure 12 depicts SST as a function of longitude in the SH at 55.5°S in the austral summer (January), autumn (April), winter (July), and spring (October). The maximum zonal gradient in each month occurs between 100° and about 170°E. Over this longitude interval the SST climbs from approximately 0.5° to 6°C in October, which is at least 0.5°C greater than the observed change over the same interval in July and approximately 1°C greater than the corresponding changes in January and April. Within this longitude range the zonal increase of SST in July and October is greatest between 145° and 170°E where an increase of about 4°C is observed (Fig. 12). This sector reflects the southward displacement of the ACC as it encounters the change in bathymetry associated with the Macquarie Rise and Campbell Plateau (Nowlin and Klinck 1986; Pook 1994). The SST pattern at lower latitudes does not display the strong west to east warming from the central Indian Ocean sector to the Tasman Sea, which is evident south of 45°S.

Hirst and Linacre (1981) argued that the month of October represents a significant minimum of mean blocking activity in the Australian region. However, this month corresponds to the time of maximum west to east SST gradient south of Australia (Fig. 12). By way of contrast, during the month of maximum blocking frequency (viz. June) the west to east SST gradient is weaker than in October (not shown). It is clear from the seasonal

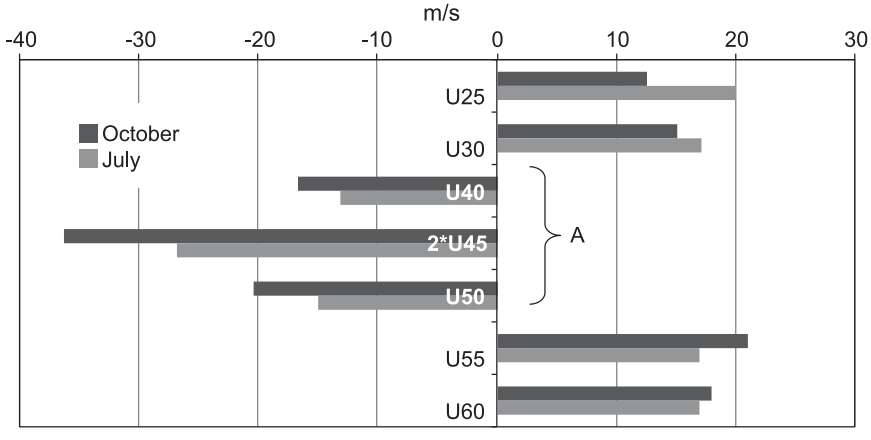

FIG. 10. The mean U components of the 500-hPa wind ($m\,s^{-1}$) in July and October along the 140°E meridian at the latitudes employed in the calculation of the BI. The three components contained within the bracket A have been shown as negative and the value at 45°S has been doubled in order to match the terms in the BI formula [see Eq. (1)]. (NCEP–NCAR Reanalysis 1 data are for the period during 1958–2009.)

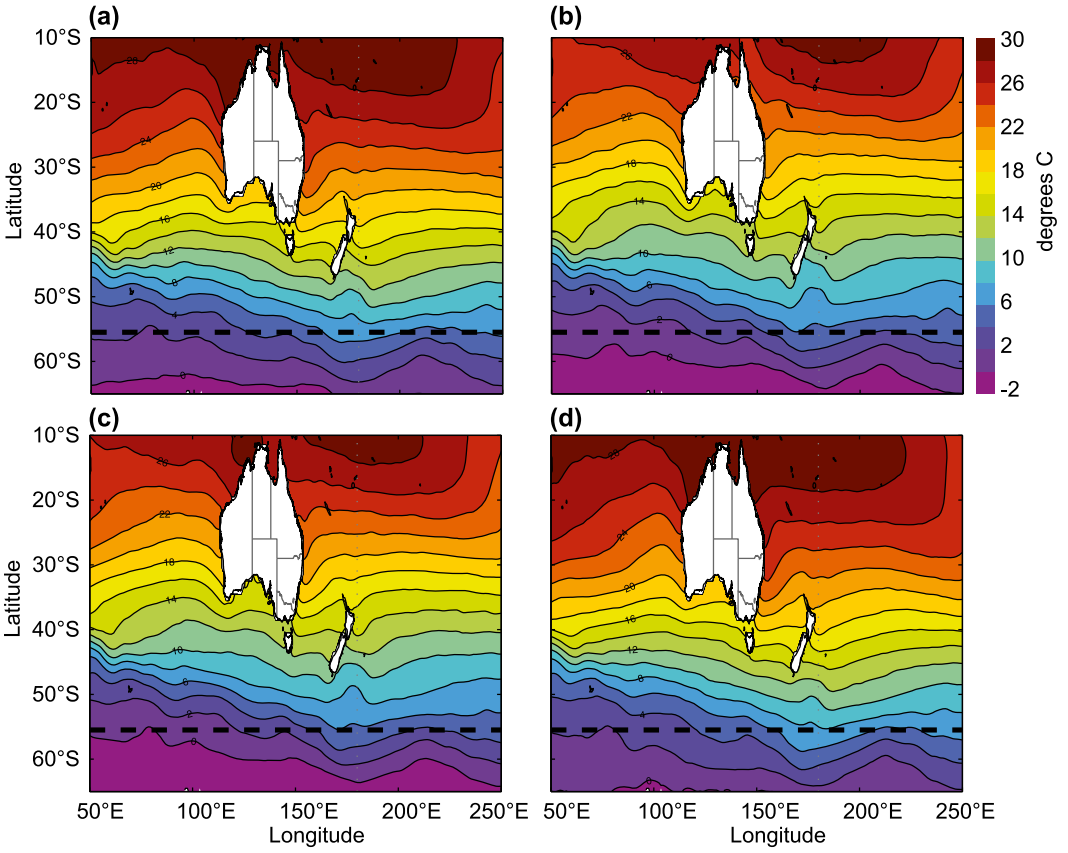

FIG. 11. Mean SST in the Southern Hemisphere (°C) for the austral (a) autumn (MAM), (b) winter (JJA), (c) spring (SON), and (d) summer (DJF). HadISST data are for the period during 1958–2009. The dashed black line along 55.5°S marks the latitude of the zonal cross section in Fig. 12.

changes of atmospheric thickness from winter to spring previously shown in Fig. 8d that the signal is dominated by warming over the Australian continent and the subtropical oceans with minimal change over the Southern Ocean. Hence, the west to east SST gradient in the Southern Ocean must be regarded as an inadequate explanation for the seasonal cycle of blocking frequency in the region. This does not mean that it is not involved in the underlying mechanism of blocking but the evidence suggests that it can only have a secondary rather than primary role in the seasonal cycle.

In contrast to the behavior of the zonal gradients of SST, the seasonal changes in meridional SST gradients are relatively large. Meridional SST gradients are communicated to the lower atmosphere and are therefore closely related to the degree of baroclinicity. Although horizontal temperature gradients have been presented here as the key influence on baroclinicity, it should be noted that Walland and Simmonds (1999) have shown that the static stability of the atmosphere plays an important role in modulating the amplitude of some climatological features in the Southern Ocean. Figure 13 reveals that the decrease in SST from the austral summer to the winter is greatest in the subtropics. It is greatest (≤ -4°C) between 30° and 35°S in the Indian Ocean sector but the region of cooling greater than 3°C in the southwest Pacific sector is more extensive, reaching the southern boundary of the Tasman Sea. The large decrease in SST in this latitude belt from summer to winter can be explained by the change from relatively light winds when the subtropical ridge is closest to the pole, to stronger westerly winds as the ridge makes its closest approach to the equator. The wind change to stronger westerlies acts to increase the depth of the mixed layer, enhance evaporative cooling, promote equatorward Ekman transport, and thus lower the SST (Dong et al. 2008). Farther south in the Southern Ocean where the change in the strength of the westerly winds is relatively minor the decreases in SST lie mainly within the range from -1° to -2°C. However, they range from -2° to -3°C south of 60°S in the sea ice zone. Simmonds and King (2004) show a similar pattern of oceanic cooling

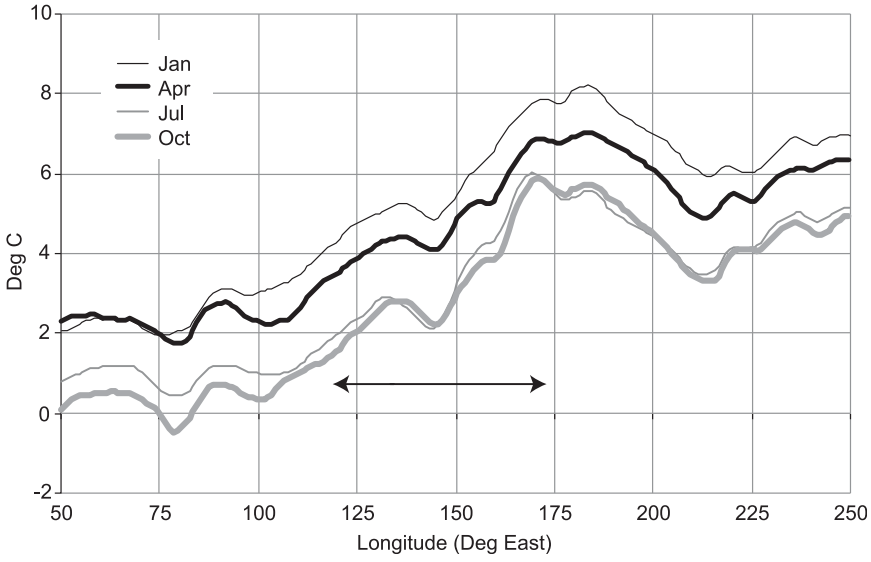

FIG. 12. Cross section of SST along 55.5°S as a function of longitude from 50° to 250°E for the months of January, April, July, and October from HadISST (during 1958–2009).

(their Fig. 3) to the summer to winter change in Fig. 13, but in their case the mean seasonal range of SST is presented, thereby taking account of lags in the ocean relative to the solar radiation cycle.

The pattern of cooling in Fig. 13 matches the pattern of shrinkage in atmospheric thickness over the oceanic region, which is depicted in Figs. 8b,c. The greatest decrease in thickness occurs in a band between 25° and 40°S and is greatly amplified over the central and southern portions of the Australian continent where surface mean temperatures decrease by between 10° and 18°C from summer to winter. It is noteworthy that in the region south of 30°S the meridional SST gradients are steeper at the lower latitudes in summer compared to winter and steeper in winter than in summer at the higher latitudes. Notwithstanding the changes in meridional temperature gradients in the ocean, Fig. 14 shows that the greatest changes in meridional gradients of surface air temperature occur over Australia and around the Antarctic continent.

5. Blocking and Australian rainfall

Risbey et al. (2009b) presented correlations between the remote climate drivers and rainfall variability in various parts of Australia and found that one or two drivers appear to be significant at any given time of year in most regions of the country. In the particular case of

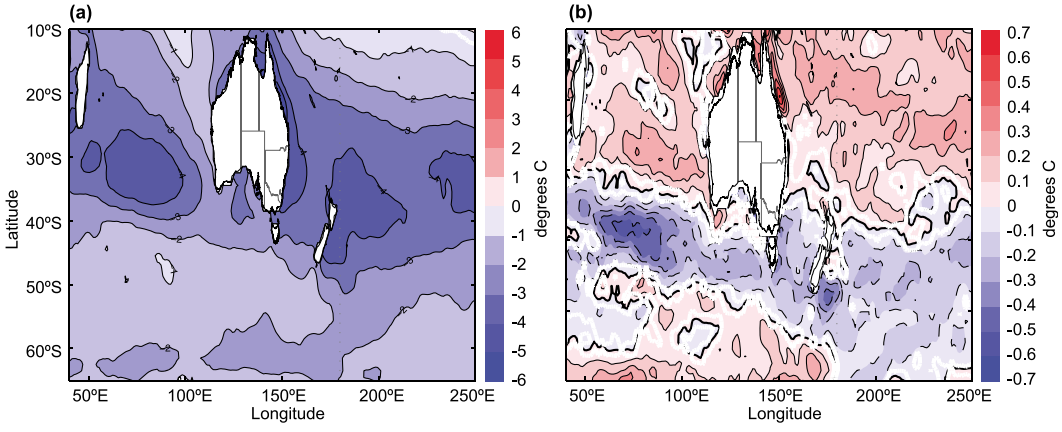

FIG. 13. The change in (a) SST (°C) and (b) meridional SST gradient (°C per degree of latitude) from the austral summer (DJF) to the austral winter (JJA) over the oceanic region from the western Indian Ocean sector to the central Pacific. (HadISST data are for the period during 1958–2009.)

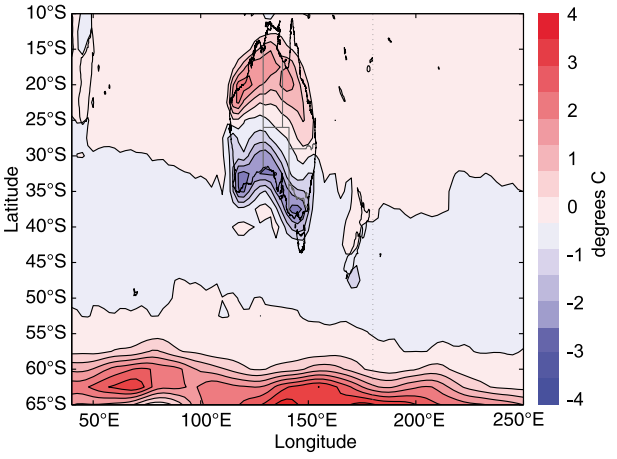

FIG. 14. Change in meridional surface air temperature gradient (°C per degree of latitude) from summer (DJF) to winter (JJA). NCEP–NCAR Reanalysis 1 data are for the period during 1958–2009 at the model sigma level 0.995 (~42 m AGL).

the southeast region it was found that autumn, winter, and spring rainfall was influenced by the phase of ENSO, the polarity of the Indian Ocean dipole (IOD), the SAM, and blocking (Risbey et al. 2009b, and references therein). The areas of influence for each of the drivers were shown to exhibit considerable variability on the decadal scale and there was evidence of large decadal variability in the association of rainfall with any given driver in a selected location. Additionally, Risbey et al. (2009b) found that blocking to the southeast of Australia is more probable during the La Niña state in the Pacific than it is in the El Niño phase. The underlying causes of decadal variability in their correlation study were not explored further by Risbey et al. (2009b). Other studies have sought to link the Pacific decadal oscillation (PDO) to rainfall variability over Australia. For example, Pezza et al. (2007) have shown that the frequency and intensity of synoptic systems at the mid- and high latitudes of the Australian region exhibit variability on the decadal scale, which is related to the phase of the PDO.

An early attempt to establish relationships between the BI and monthly rainfall in Australia from an approximately 14-yr dataset was regarded as disappointing (Ohis 1980). However, based on more than five decades of data, Risbey et al. (2009b) have presented the instantaneous correlations between the BI at 140°E and rainfall over Australia in the individual seasons. Their Fig. 13 shows that the highest positive correlations (~0.7) with rainfall over southeastern Australia occur in winter and spring while maximum negative correlations with rainfall in southwestern Tasmania (approximately −0.5) occur in autumn and spring. In Fig. 15 we demonstrate the correlation between the BI and Australian rainfall for the austral seasons at three meridians (120°, 140°, and 150°E) with the linear trends removed from the time series. The correlations at 130°E are not shown as they are similar to the results for 140°E.

The highest correlation (slightly) is found to the west of the meridian for which the BI is calculated in each case. The hypothesis advanced here is that the significant correlation of rainfall with blocking is a consequence of the high frequency of occurrence of upper troughs and cutoff lows forming to the north of the primary blocking anticyclone, thus completing the dipole structure (e.g., see Fig. 1). Clearly, this effect is found to extend throughout much of New South Wales, Australia, and even to southern and central Queensland, Australia. For the summer season the correlation between the BI and rainfall is apparently a more complex relationship than in the other seasons.

Pook et al. (2006) have demonstrated that cutoff lows are responsible for approximately 50% of growing season rainfall in northwestern Victoria, Australia, and in a subsequent study, Pook et al. (2009) showed the dominant role played by cutoff lows in the onset of autumn rain. In the Central Wheatbelt of Western Australia, Pook et al. (2012) found that cutoff lows contribute approximately 33% of growing season rainfall. Given the close relationship between blocking and cutoff lows, any decline in blocking activity may be expected to be accompanied by a decrease in cutoff low rainfall. Risbey et al. (2012) report that declining rainfall from cutoff lows coupled to a decline in blocking activity was the largest contributor to the reduction in rainfall in southeastern Australia during the major drought from 1996 to 2009. Composites of rainfall over southern Australia during the growing season for high (≥1 standard deviation) and low (≤−1 standard deviation) mean values of the BI at 140°E for the April–October period do indeed reveal that above average rainfall is found in the high BI cluster and relatively low rainfall is associated with the low BI group (see Fig. 16).

To relate blocking to rainfall specifically associated with particular types of synoptic systems, rainfall over southern Australia has been partitioned according to its synoptic origin in the manner of Pook et al. (2006, 2012). They categorized synoptic systems producing rainfall into three main classes: frontal types associated with Southern Ocean depressions, cutoff lows, and a combined category designated as ''others'' that included various airstreams, waves in the easterlies, and several trough types. Figure 17 shows the correlation between ''cutoff low'' rainfall during the growing season over the southern mainland and the blocking index at a selection of meridians from 120° to 150°E. The results are derived

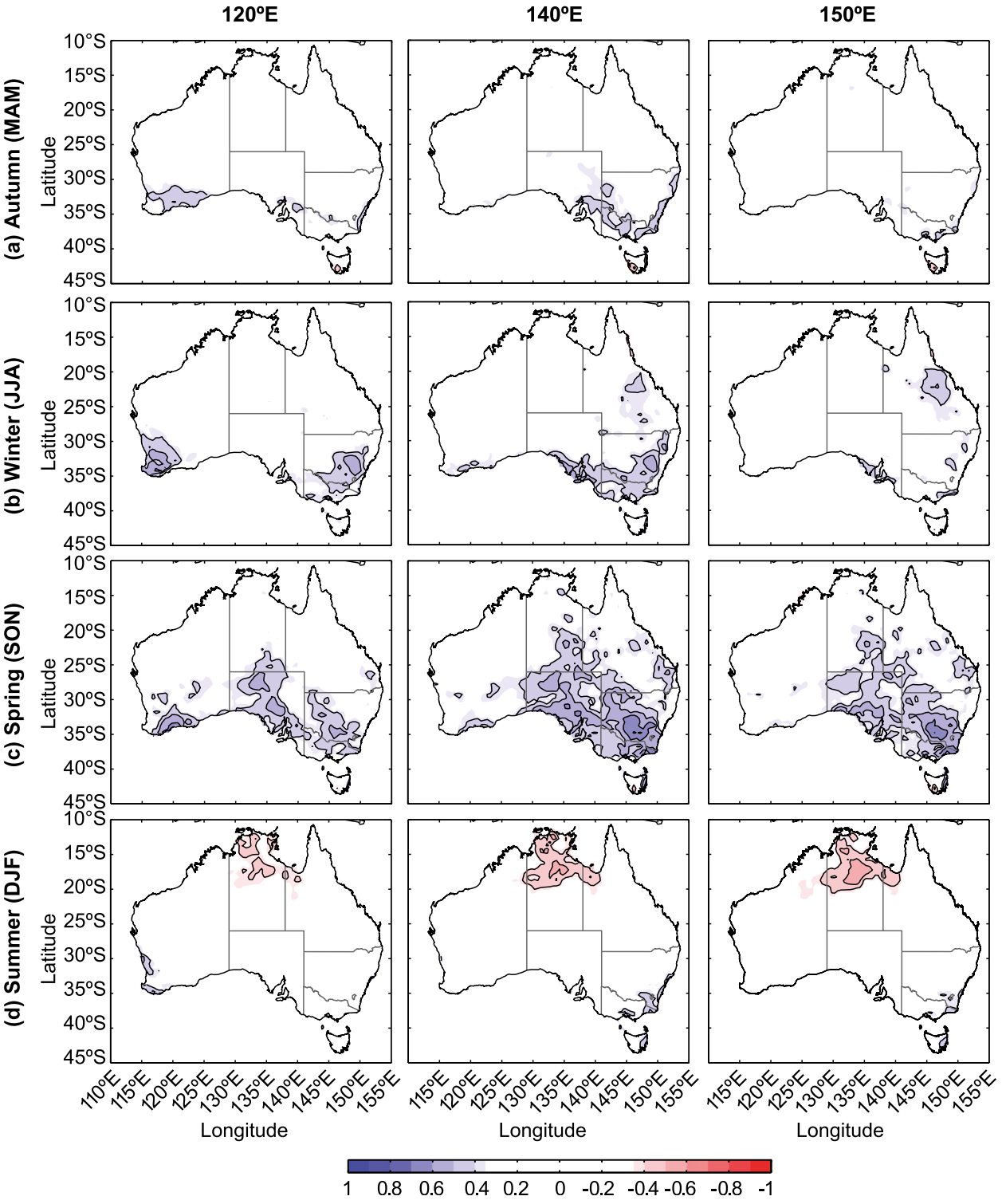

FIG. 15. Correlations between the BI and AWAP rainfall for the austral seasons of (a) autumn (MAM), (b) winter (JJA), (c) spring (SON), and (d) summer (DJF) at 120°, 140°, and 150°E. Shading indicates confidence at the 99% level. The period of the analysis is from 1958 to 2009 and the data have been detrended. The two-sided significance of the correlations has been determined using a conservative statistic appropriate to both small and large numbers of samples [Press et al. (1986), p. 486, Eq. (13.7.5)].

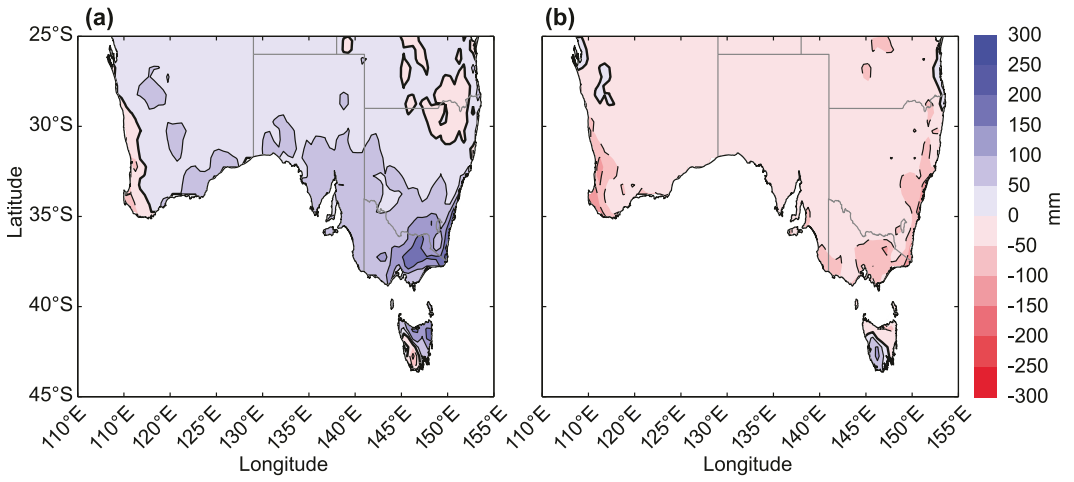

FIG. 16. Composites of rainfall anomalies for the April–October "growing" season for years of (a) anomalously high BI at 140°E and (b) anomalously low BI at 140°E.

for the period from 1965 to 2009 and are based on two analysis boxes, one for southeastern Australia (see Pook et al. 2006) and one for the southwest of the Australian continent (see Pook et al. 2012) . The analysis boxes have been included in Fig. 17. Shading indicates correlation coefficients exceeding 0.38 (n = 45), which are significant at the 99% confidence level. Although the rainfall data sampled are year to year seasonal averages, Simmonds and Hope (1997) have shown that the data may be weakly correlated from year to year and this effect is likely to reduce the effective degrees of freedom.

Cutoff rainfall and the BI at meridians from 120° to 140°E are highly correlated over inland parts of southeastern Australia and southwestern Australia (see Figs. 17a–c) but the area of significant correlation between the BI at 150°E and cutoff rainfall is mainly confined to the state of South Australia (Fig. 15d). There is no apparent correlation between the BI and rainfall of frontal origin at the 99% confidence level (not shown).

6. Conclusions

This paper follows previous studies in contending that the strong predisposition to blocking in the Australian region in the winter half of the year derives partially from the relatively large seasonal decreases in temperature over continental Australia from summer to winter but expatiates upon this argument by invoking major additional influences. These include the large seasonal cooling signal of the Antarctic continent and the smaller, but nevertheless significant, decreases in SST in the subtropical ocean. The seasonal influences occur within the favorable background state for blocking in the southwest Pacific region of the SH, which is induced by the regional topography and the SST configuration in the Southern Ocean. The response in the atmospheric column to the seasonal surface temperature changes is reflected in large changes in the 1000–500-hPa thickness over southern Australia and near the Antarctic coast and smaller but significant decreases in thickness over the subtropical ocean. By way of contrast, the smallest seasonal changes in the SST occur at high latitudes (south of 50°S) of the well-mixed Southern Ocean where decreases in thickness are minimal. The resulting changes in thermal wind explain the observed changes in the position and strength of the dominant jet streams from summer to winter.

The Australian BoM blocking index (BI) is the primary measure of blocking adopted in this paper. Overall, the BI is a useful climatological measure of blocking but there is a strong seasonal cycle to consider. The BI is compared with the Tibaldi–Molteni Index (TMBI) and it is found that stringent application of the TMBI in the SH allows only relatively few events to qualify as "blocking." Some relaxation of the TMBI conditions is required for the winter half of the year in order to provide a more useful measure. Nevertheless, the TMBI may be preferable to the BI as an indicator of summer blocking events. Overall, no single measure of blocking can provide the ideal identification of blocking in every situation but recent attempts to investigate new ways of characterizing the phenomenon appear promising. In particular, dynamically based assessments of blocking may offer advantages over current empirical measures.

Significant correlations between the BI at Australian longitudes and seasonal rainfall have been demonstrated in southern and central Australia for the austral autumn, winter, and spring. The highest correlations

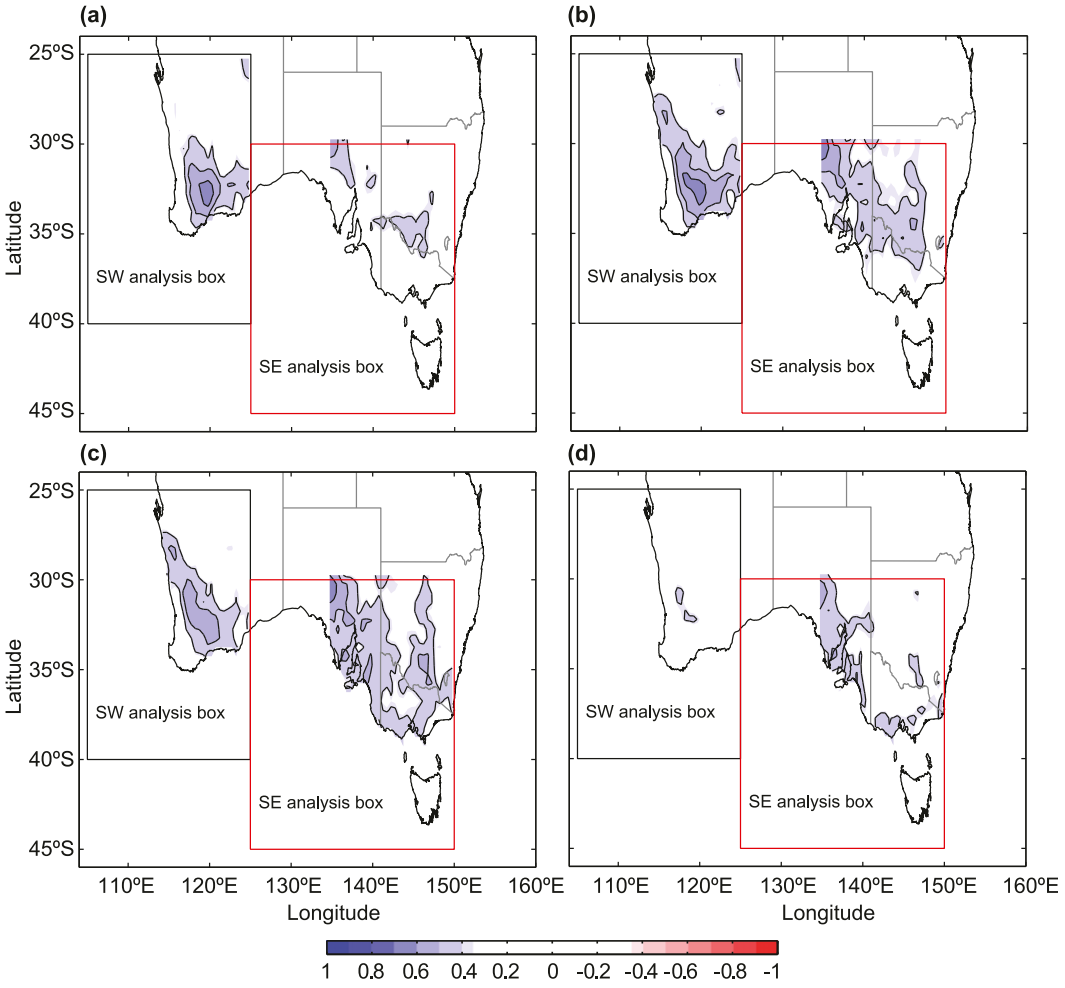

FIG. 17. Correlations between the BI and rainfall from cutoff low systems for the southern Australian growing season (AMJJASO) at (a) 120°, (b) 130°, (c) 140°, and (d) 150°E. Shading indicates confidence at the 99% level according to the method of Press et al. (1986) [p. 486, Eq. (13.7.5)]. The period of the analysis is from 1965 to 2009 and the data have been detrended.

occur well inland. However, only patchy positive correlations have been found in the south during summer and unexplained negative correlations are apparent in the central tropical north.

By decomposing the rainfall into its contributions from identifiable synoptic types during the April–October growing season in southern Australia it has been shown that the high correlation between blocking and rainfall is explained by the component of rainfall associated with cutoff lows. On the other hand, there is no significant correlation between the BI and rainfall from Southern Ocean fronts.

The seasonal cycle of atmospheric blocking in the Australian sector of the SH explains features of the seasonal and interannual variability in rainfall over southern Australia. The connection to rainfall is provided by the symbiotic association between high-latitude blocking anticyclones and the formation of upper troughs and cutoff lows over southern Australia as the cyclonic component of the blocking pattern. This interaction offsets the suppression by blocking of rain from Southern Ocean fronts, particularly in the southeast.

Acknowledgments. This work was partly funded by the Managing Climate Variability Program of the Australian Government, which is managed by the Grains Research and Development Corporation. CCU received support from the Australian Research Council through funding awarded to the Centre of Excellence for Climate System Science. Drs. Andrew Dowdy and Terence O'Kane provided valuable comments on an earlier draft of the manuscript and the paper has been improved by the constructive comments of three reviewers. We gratefully

acknowledge use of the SODA reanalysis product, accessed through the IRI Data Library.

REFERENCES

Baines, P. G., 1983: A survey of blocking mechanisms, with application to the Australian region. *Aust. Meteor. Mag.,* **31,** 27–36.

Bals-Elsholz, T. M., E. H. Atallah, L. F. Bosart, T. A. Wasula, M. J. Cempa, and A. R. Lupo, 2001: The wintertime Southern Hemisphere split jet: Structure, variability and evolution. *J. Climate,* **14,** 4191–4215.

Barriopedro, D., R. Garcia-Herrera, A. R. Lupo, and E. Hernandez, 2006: A climatology of Northern Hemisphere blocking. *J. Climate,* **19,** 1042–1063.

Bradshaw, B., 1997: Instrumental and observing networks. *Windows on Meteorology: Australian Perspective,* E. K. Webb, Ed., CSIRO Publishing, 127–141.

Bromwich, D. H., and T. R. Parish, 1998: Meteorology of the Antarctic. *Meteorology of the Southern Hemisphere, Meteor. Monogr*., No. 49, Amer. Meteor. Soc., 175–200.

Carton, J. A., and B. S. Giese, 2008: A reanalysis of ocean climate using Simple Ocean Data Assimilation (SODA). *Mon. Wea. Rev.,* **136,** 2999–3017.

Charney, J. G., and J. G. DeVore, 1979: Multiple flow equilibria in the atmosphere and blocking. *J. Atmos. Sci.,* **36,** 1205–1216.

——, J. Shukla, and K. C. Mo, 1981: Comparison of a barotropic blocking theory with observation. *J. Atmos. Sci.,* **38,** 762–779.

Coughlan, M. J., 1983: A comparative climatology of blocking action in the two hemispheres. *Aust. Meteor. Mag.,* **31,** 3–13.

Dong, S., J. Sprintall, S. T. Gille, and L. Talley, 2008: Southern Ocean mixed-layer depth from Argo float profiles. *J. Geophys. Res.,* **113,** C06013, doi:10.1029/2006JC004051.

Foley, J. C., 1956: 500 mb contour patterns associated with the occurrence of widespread rains in Australia. *Aust. Meteor. Mag.,* **13,** 1–18.

Frederiksen, J. S., 1983: The onset of blocking and cyclogenesis: Linear theory. *Aust. Meteor. Mag.,* **31,** 15–26.

Gentilli, J., 1971: The main climatological elements. *Climates of Australia and New Zealand,* J. Gentilli, Ed., Vol. 13, *World Survey of Climatology,* Elsevier, 119–188.

Gill, A. E., 1982: *Atmosphere–Ocean Dynamics.* Academic Press, 662 pp.

Gong, D., and S. Wang, 1999: Definition of Antarctic oscillation index. *Geophys. Res. Lett.,* **26,** 459–462.

Griffiths, M., M. J. Reeder, D. J. Low, and R. A. Vincent, 1998: Observations of a cut-off low over southern Australia. *Quart. J. Roy. Meteor. Soc.,* **124,** 1109–1132.

Hill, H. W., 1969: A cyclonic disturbance in the upper troposphere associated with widespread rain over southeastern Australia. Tech. Note 92, WMO 228, TP 122, *Symp. Hydrological Forecasting,* Surfers Paradise, Queensland, Australia, WMO, 37–50.

Hirst, A. C., and E. T. Linacre, 1981: Trends in the blocking of high-pressure systems in the Australian region. *Search,* **12,** 409–411.

Hopkins, L. C., and G. J. Holland, 1997: Australian heavy-rain days and associated east coast cyclones: 1958–92. *J. Climate,* **10,** 621–635.

Hurrell, J. W., H. van Loon, and D. J. Shea, 1998: The mean state of the troposphere. *Meteorology of the Southern Hemisphere, Meteor. Monogr.,* No. 49, Amer. Meteor. Soc., 1–46.

Jeffrey, S. J., J. O. Carter, K. M. Moodie, and A. R. Beswick, 2001: Using spatial interpolation to construct a comprehensive archive of Australian climate data. *Environ. Modell. Software,* **16** (4), 309–330.

Jones, D. A., W. Wang, and R. Fawcett, 2009: High-quality spatial climate data-sets for Australia. *Aust. Meteor. Oceanogr. J.,* **58,** 233–248.

Kalnay, E., and Coauthors, 1996: The NCEP/NCAR 40-Year Reanalysis Project. *Bull. Amer. Meteor. Soc.,* **77,** 437–471.

King, J. C., and J. Turner, 1997: *Antarctic Meteorology and Climatology.* Cambridge University Press, 409 pp.

Kistler, R., and Coauthors, 2001: The NCEP–NCAR 50-Year Reanalysis: Monthly means CD-ROM and documentation. *Bull. Amer. Meteor. Soc.,* **82,** 247–267.

Langford, J. C., 1960: Aspects of circulation and analysis of the Southern Ocean. *Antarctic Meteorology,* Pergamon Press, 256–273.

Lejenäs, H., 1984: Characteristics of southern hemisphere blocking as determined from a time series of observational data. *Quart. J. Roy. Meteor. Soc.,* **110,** 967–979.

Majda, A., C. Franzke, A. Fischer, and D. Crommelin, 2006: Distinct atmospheric regimes despite nearly Gaussian statistics: A paradigm model. *Proc. Natl. Acad. Sci. USA,* **103,** 8309–8314.

Marshall, A. G., D. Hudson, H. H. Hendon, M. J. Pook, O. Alves, and M. C. Wheeler, 2013: Simulation and prediction of blocking in the Australian region and its influence on intraseasonal rainfall in POAMA-2. *Climate Dyn.,* doi:10.1007/s00382-013-1974-7, in press.

Massom, R. A., M. J. Pook, J. C. Comiso, N. Adams, J. Turner, T. Lachlan-Cope, and T. T. Gibson, 2004: Precipitation over the interior East Antarctic ice sheet related to midlatitude blocking-high activity. *J. Climate,* **17,** 1914–1928.

Meneghini, B., I. Simmonds, and I. Smith, 2007: Association between Australian rainfall and the Southern Annular Mode. *Int. J. Climatol.,* **27,** 109–121.

Mills, G. A., and B.-J. Wu, 1995: The 'Cudlee Creek' flash flood—An example of synoptic-scale forcing of a mesoscale event. *Aust. Meteor. Mag.,* **44,** 201–218.

Nowlin, W. D., Jr., and J. M. Klinck, 1986: The physics of the Antarctic Circumpolar Current. *Rev. Geophys.,* **24,** 469–491.

Ohis, L. F., 1980: On the influence of blocking indices on rainfall in the Australian region. Meteorological Note 80, Australian Bureau of Meteorology, 21 pp.

O'Kane, T., J. Risbey, C. Franzke, I. Horenko, and D. Monselesan, 2013: Changes in the metastability of the midlatitude Southern Hemisphere circulation and the utility of nonstationary cluster analysis and split-flow blocking indices as diagnostic tools. *J. Atmos. Sci*., **70,** 824–842.

Palmer, T. N., F. J. Doblas-Reyes, A. Weisheimer, and M. J. Rodwell, 2008: Toward seamless prediction; Calibration of climate change projections using seasonal forecasts. *Bull. Amer. Meteor. Soc.,* **89,** 459–470.

Pezza, A. B., I. Simmonds, and J. Renwick, 2007: Southern Hemisphere cyclones and anticyclones: Recent trends and links with decadal variability in the Pacific Ocean. *Int. J. Climatol.,* **27,** 1403–1419.

Pook, M. J., 1992: A note on the variability of the mid-tropospheric flow over the Southern Ocean in the Australian region. *Aust. Meteor. Mag.,* **40,** 169–177.

——, 1994: Atmospheric blocking in the Australasian region in the Southern Hemisphere winter. Ph.D. thesis, University of Tasmania, 168 pp.

——, and L. Cowled, 1999: On the detection of weather systems over the Antarctic interior in the FROST analyses. *Wea. Forecasting,* **14,** 920–929.

——, and T. Gibson, 1999: Atmospheric blocking and storm tracks during SOP-1 of the FROST Project. *Aust. Meteor. Mag.*, Special Edition, 51–60.

——, P. C. McIntosh, and G. A. Meyers, 2006: The synoptic decomposition of cool-season rainfall in the southeastern Australian cropping region. *J. Appl. Meteor. Climatol.,* **45,** 1156–1170.

——, S. Lisson, J. Risbey, C. C. Ummenhofer, P. C. McIntosh, and M. Rebbeck, 2009: The autumn break for cropping in southeast Australia: Trends, synoptic influences and impacts on wheat yield. *Int. J. Climatol.,* **29,** 2012–2026.

——, J. Risbey, and P. McIntosh, 2010: East coast lows, atmospheric blocking and rainfall: A Tasmanian perspective. *IOP Conf. Ser.: Earth Environ. Sci.*, **11,** 012011, doi:10.1088/1755-1315/11/1/012011.

——, ——, and ——, 2012: The synoptic climatology of cool-season rainfall in the Central Wheatbelt of Western Australia. *Mon. Wea. Rev.,* **140,** 28–43.

Press, W. H., B. P. Flannery, S. A. Teukolsky, and W. T. Vetterling, 1986: *Numerical Recipes: The Art of Scientific Computing.* Cambridge University Press, 818 pp.

Qi, L., L. M. Leslie, and S. X. Zhao, 1999: Cut-off low pressure systems over southern Australia: Climatology and case study. *Int. J. Climatol.,* **19,** 1633–1649.

Radok, U., 1971: The Australian region and the general circulation of the Southern Hemisphere. *Climates of Australia and New Zealand,* J. Gentilli, Ed., Vol. 13, *World Survey of Climatology,* Elsevier, 13–33.

Rayner, N. A., D. E. Parker, E. B. Horton, C. K. Folland, L. V. Alexander, D. P. Rowell, E. C. Kent, and A. Kaplan, 2003: Global analyses of sea surface temperature, sea ice, and night marine air temperature since the late nineteenth century. *J. Geophys. Res.,* **108,** 4407, doi:10.1029/2002JD002670.

Renwick, J. A., 1998: ENSO-related variability in the frequency of South Pacific blocking. *Mon. Wea. Rev.,* **126,** 3117–3123.

——, 2005: Persistent positive anomalies in the Southern Hemisphere circulation. *Mon. Wea. Rev.,* **133,** 977–988.

Rex, D. F., 1950: Blocking action in the middle troposphere and its effect upon regional climate. Part I: An aerological study of blocking action. *Tellus,* **2,** 196–211.

Risbey, J., M. J. Pook, P. McIntosh, C. Ummenhofer, and G. Meyers, 2009a: Characteristics and variability of synoptic features associated with cool season rainfall in southeastern Australia. *Int. J. Climatol.,* **29,** 1595–1613, doi:10.1002/joc.1775.

——, ——, ——, M. Wheeler, and H. Hendon, 2009b: On the remote drivers of rainfall variability in Australia. *Mon. Wea. Rev.,* **137,** 3233–3253.

——, P. C. McIntosh, and M. J. Pook, 2012: Synoptic components of rainfall variability and trends in southeast Australia. *Int. J. Climatol.*, **33,** 2459–2472, doi:10.1002/joc.3597.

Schalge, B., R. Blender, and K. Fraedrich, 2011: Blocking detection based on synoptic filters. *Adv. Meteor.,* **2011,** 717812, doi:10.1155/2011/717812.

Simmonds, I., and P. Hope, 1997: Persistence characteristics of Australian rainfall anomalies. *Int. J. Climatol.,* **17,** 597–613.

——, and J. C. King, 2004: Global and hemispheric climate variations affecting the Southern Ocean. *Antarct. Sci.,* **16,** 401–413.

Sinclair, M. R., 1996: A climatology of anticyclones and blocking for the Southern Hemisphere. *Mon. Wea. Rev.,* **124,** 245–263.

Sturman, A., and N. Tapper, 1996: *The Weather and Climate of Australia and New Zealand.* Oxford University Press, 476 pp.

Taljaard, J. J., 1972: Synoptic meteorology of the Southern Hemisphere. *Meteorology of the Southern Hemisphere, Meteor. Monogr.,* No. 35, Amer. Meteor. Soc., 139–213.

Tibaldi, S., and F. Molteni, 1990: On the operational predictability of blocking. *Tellus,* **42A,** 343–365.

——, E. Tosi, A. Navarra, and L. Pedulli, 1994: Northern and Southern Hemisphere seasonal variability of blocking frequency and predictability. *Mon. Wea. Rev.,* **122,** 1971–2003.

Tobin, S., and T. C. L. Skinner, 2012: Seasonal climate summary Southern Hemisphere (Autumn 2011): One of the strongest La Niña events on record begins to decline. *Aust. Meteor. Oceanogr. J.,* **62,** 39–50.

Trenberth, K. E., and K. C. Mo, 1985: Blocking in the Southern Hemisphere. *Mon. Wea. Rev.,* **113,** 3–21.

Ummenhofer, C. C., P. C. McIntosh, M. J. Pook, and J. S. Risbey, 2013: Impact of surface forcing on Southern Hemisphere atmospheric blocking in the Australia–New Zealand sector. *J. Climate,* **26,** 8476–8494.

van Loon, H., 1956: Blocking action in the Southern Hemisphere. Part 1. *Notos,* **5,** 171–175.

Walland, D., and I. Simmonds, 1999: Baroclinicity, meridional temperature gradients, and the southern Semiannual Oscillation. *J. Climate,* **12,** 3376–3382.

Walsh, K. J. E., I. Simmonds, and M. Collier, 2000: Sigma-coordinate calculation of topographically forced baroclinicity around Antarctica. *Dyn. Atmos. Oceans,* **33,** 1–29.

Watson, J. S., and S. J. Colucci, 2002: Evaluation of ensemble predictions of blocking in the NCEP global spectral model. *Mon. Wea. Rev.,* **130,** 3008–3021.

Wiedenmann, J. M., A. R. Lupo, I. I. Mokhov, and E. A. Tikhonova, 2002: The climatology of blocking anticyclones for the Northern and Southern Hemispheres: Block intensity as a diagnostic. *J. Climate,* **15,** 3459–3473.

Wright, A. D. F., 1974: Blocking action in the Australian region. Tech. Rep. 10, Bureau of Meteorology, Australia, 29 pp.

Zidikheri, M. J., J. S. Frederiksen, and T. J. O'Kane, 2007: Multiple equilibria and atmospheric blocking. *Frontiers in Turbulence and Coherent Structures,* J. Denier and J. S. Frederiksen, Eds., *Proceedings of the COSNet/CSIRO Workshop on Turbulence and Coherent Structures in Fluids, Plasmas and Nonlinear Media,* World Scientific, 59–85.